Eur. Phys. J. Appl. Phys. **31**, 87–93 (2005)
DOI: 10.1051/epjap:2005044

THE EUROPEAN PHYSICAL JOURNAL APPLIED PHYSICS

Enhancement of the optical and electrical properties of ITO thin films deposited by electron beam evaporation technique

H.M. Ali[a], H.A. Mohamed, and S.H. Mohamed

Physics Department, Faculty of Science, South Valley University, 82524 Sohag, Egypt

Received: 10 September 2004 / Received in final form: 28 February 2005 / Accepted: 12 April 2005
Published online: 11 July 2005 –

Abstract. Indium tin oxide (ITO) is widely utilized in numerous industrial applications due to its unique combined properties of transparency to visible light and electrical conductivity. ITO films were deposited on glass substrates by an electron beam evaporation technique at room temperature from bulk samples, with different thicknesses. The film with 1500 Å thick was selected to perform annealing in the temperature range of 200–400 °C and annealing for varying times from 15 to 120 min at 400 °C. The X-ray diffraction of the films was analyzed in order to investigate its dependence on thickness, and annealing. Electrical and optical measurements were also carried out. Transmittance, optical energy gap, refractive index, carrier concentration, thermal emissivity and resistivity were investigated. It was found that the as-deposited films with different thicknesses were highly absorbing and have relatively poor electrical properties. The films become opaque with increasing the film thickness. After thermal annealing, the resistance decreases and a simultaneous variation in the optical transmission occurs. A transmittance value of 85.5% in the IR region and 82% in the visible region of the spectrum and a resistivity of $2.8 \times 10^{-4}\,\Omega$ Cm were obtained at annealing temperature of 400 °C for 120 min.

PACS. 61.10.-i X-ray diffraction and scattering – 78.66.-w Optical properties of specific thin films – 73.61.-r Electrical properties of specific thin films – 73.50.-h Electronic transport phenomena in thin films

1 Introduction

Although partial transparency, with acceptable reduction in conductivity, can be obtained for very thin metallic films, high transparency and simultaneously high conductivity can not be obtained in intrinsic stoichiometric materials. The only way this can be achieved is by creating electron degeneracy in a wide band gap ($E_g > 3.5$ eV or more for visible radiation) material by introducing non-stoichiometry and/or appropriate dopants in a controlled manner. These conditions can be conveniently met for ITO as well as a number of other materials.

Semiconducting (ITO) material in thin film form has received much attention due to its wide band gap [1] and high IR reflectivity properties [2]. ITO thin films are widely utilized as an essential part of many optoelectronic devices, such as flat panel displays, thin film transistors, sensors, liquid crystal displays, solar cells, energy efficient window system because of their unique properties of high electrical conductivity and high optical transparency in the visible region [3–4]. Its use in energy efficient window system is mainly due to its high reflectivity in the NIR region. This is also useful for devices where optics of low thermal emissivity [5,6] properties are required.

Several methods, such as sputtering [7–10] thermal evaporation [11,12], spray pyrolysis [13], screen printing [14], sol-gel [15] and pulsed laser deposition (PLD) [16], etc. have been followed for the deposition of ITO films on glass substrates.

In order to obtain optimal characteristics of TCO (transparent conductive oxides) films, the parameters such as substrate temperature, thickness, dopants, heat treatment (annealing temperature and time) and other deposition conditions have to be optimized.

In this study, results obtained by preparing coating by electron beam technique while varying film thickness and different heat treatments are described.

We were primarily interested in determining the correlation between optical and electronic properties that we have observed experimentally.

2 Experimental details

ITO films were prepared by electron beam evaporation technique from a highly pure (99.999%) cold pressed powder of 90 wt% In_2O_3 and 10 wt% SnO_2. In order to increase the diffusion process and consequently improve the homogeneity of the material, the tablets were heated up to 800 °C for 3 h. Thin films of the prepared In_2O_3:SnO_2

[a] e-mail: hazem95@yahoo.com

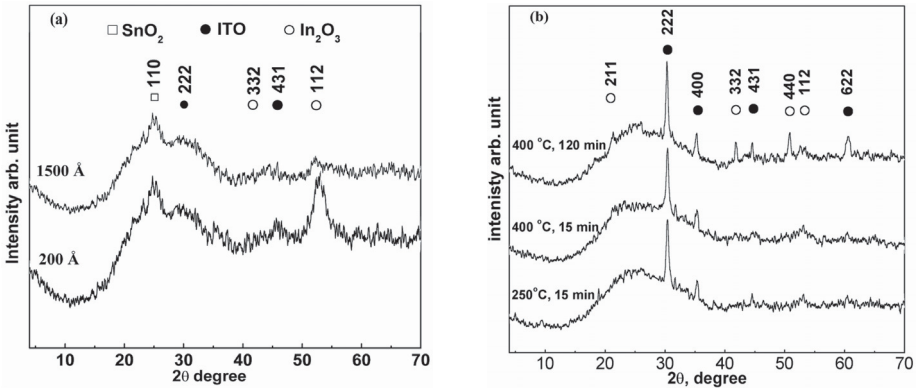

Fig. 1. X-ray diffraction of ITO thin films as a function of film thickness (a) and as a function of annealing temperature and time (b).

tablet were deposited onto ultrasonically cleaned glass substrates at 2×10^{-5} torr using Edwards high vacuum coating unit model E306A. The film thickness and deposition rate [10 nm/min] were controlled by means of a digital film thickness monitor model TM200 Maxtek. Investigations of the microstructure were carried out using an X-ray diffractometer (Philips model PW 1710).

A Jasco V-570 UV-visible-NIR spectrophotometer was employed to record the transmission and reflection spectra over the wavelength range 200–2500 nm at normal incidence. Optical parameters namely absorption coefficient (α), refractive index (n), and extinction coefficient (k) were calculated as described elsewhere [17].

The film resistivity was measured in the 80–475 K temperature range by means of a variable temperature liquid nitrogen cryostat (Oxford DN - 1710) combined with a programmable temperature controller (Oxford ITC4) and a digital Keithley 614 electrometer.

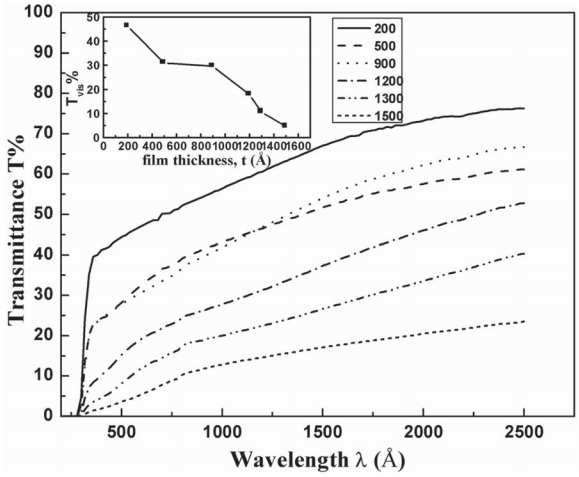

Fig. 2. The spectra of transmittance of ITO films in the wavelength range from 200 to 2500 nm for different film thickness.

3 Results and discussion

Figure 1 shows the X-ray diffraction patterns of ITO films deposited under different conditions. From Figure 1a it is quite clear that the films exhibit an amorphous structure. However diffraction peaks SnO_2 (110), In_2O_3 (332), (112) and ITO (222) and (431) were found in the amorphous matrix of the 200 Å thick film and with changed intensities also in the film with a thickness of 1500 Å. Surprisingly, the intensity of the (112) In_2O_3 peak decreased with increasing the film thickness from 200 Å to 1500 Å, indicating that the local ordering is changed with film thickness. Figure 1b shows the XRD patterns of 1500 Å thick ITO films after annealing at 250 °C and 400 °C for 15 min as well as for 120 min at 400 °C. The ITO thin films are polycrystalline and with cubic structure, since (222) and (400) oriented peaks, characteristic of a cubic structure, are present on the diffractograms. The intensities of the four major peaks, (222), (400), (440) and (622) of ITO film, were significantly affected by annealing, having maximum intensity after annealing at $T_{an} = 400$ °C for 120 min.

The films become opaque with increasing the film thickness. This opaqueness has been attributed to unoxidised Sn grains on the ITO surface as a result of instability due to absence of sufficient oxygen during deposition [18,19].

Figure 2 represents the transmittance (T) in the wavelength range from 200 to 2500 nm for different film thickness of ITO thin films in the range of 200–1500 Å and the transmittance in the visible range as a function of the film thickness. It is evident that the transmittance decreases with increasing the film thickness. This is due to the increase of opaqueness, indicating the oxygen vacancies. It can also be noted that the resistivity decreased with increasing the film thickness as shown in Figure 3. This is may be attributed to the increase of carriers mobility listed in Table 1. The resistivity attains its minimum value for 1500 Å thick film ($1.6 \times 10^{-2}\,\Omega$ cm).

The temperature dependence of the electrical conductivity $\sigma(T)$ for films having thickness $t = 200$, 500, 900, 1200, 1300 and 1500 Å in the range of temperature from 80 to about 475 K is shown in Figure 4a. Two distinct regions of $\sigma(T)$ corresponding to low and high temperature ranges are observed. In high temperature region (375–475 K) the abrupt increase in σ means that the conduction is

Table 1. The parameters of activation energy ΔE and σ_0, the density of localized states $N(E_F)$, the free carrier concentration N, mobility carriers μ and hopping parameters $\sigma_0^{\backslash}, T_0, R$ and W for ITO thin films as a function of film thickness.

Thickness (Å)	ΔE (meV)	$10^{-2}\sigma_0$ (Ω^{-1} cm^{-1})	$N(E_F)$ (eV^{-1} cm^{-3})	$10^{-20}N$ (cm^{-3})	μ (cm^2/V s)	$10^{-3}\sigma_0^{\backslash}$ (Ω^{-1} cm^{-1} K$^{1/2}$)	$10^{-3}T_0$ (K)	$10^{7}R$ (cm)	$10^{2}W$ (eV)
200	38.5	0.156	4.03×10^{17}	2.44	0.08585	0.183	0.953	14	23.57
500	33.6	0.504	4.43×10^{19}	1.33	0.71004	0.860	1.093	4.2	7.25
900	22.2	0.135	3.13×10^{18}	1.67	0.21202	0.355	1.097	8.2	14.06
1200	37.6	0.592	1.89×10^{20}	1.22	0.68221	1.189	2.841	2.9	5.04
1300	23.0	1.25	3.91×10^{21}	0.12	26.13985	3.651	1.453	1.4	2.36
1500	38.7	2.82	4.93×10^{21}	0.1	39.01373	4.007	1.320	1.3	2.23

Table 2. Variations of the optical band gap E_g, the average values of n and K in the visible spectral region, thermal emissivity and the mobility carriers with different annealing time.

Annealing time	E_g (eV)	n_{vis}	K_{vis}	Thermal emissivity	μ (cm^2/V s)
15	3.564	2.55	0.025	0.104	57.01
30	3.566	2.774	0.014	0.085	76.49
45	3.582	3.03	0.013	0.103	52.07
60	3.589	3.41	0.013	0.104	94.85
120	3.588	4.12	0.009	0.091	184.24

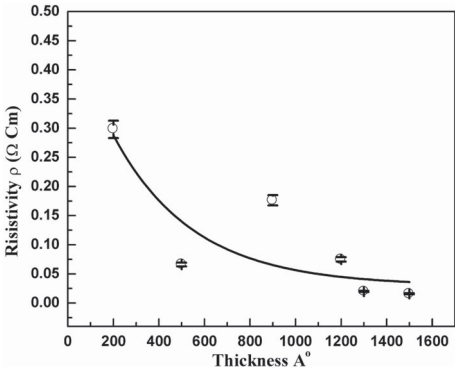

Fig. 3. Plot of thickness dependent electrical resistivity for as-deposited ITO thin films.

thermally activated and can be described by the relation:

$$\sigma = \sigma_0 \exp(-\Delta E/kT)$$

where ΔE is the corresponding activation energy and σ_0 is the pre-exponential factor. In the wide low temperature region (80–375 K), $\sigma(T)$ exhibit relatively less thermal activation, which is characterized by hopping conduction between the localized states even at values of T over room temperature. Good fits to straight lines for the relation $\ln\sigma\sqrt{T}$ versus $(1/T)^{1/4}$ are shown in Figure 4b. These plots seemed to verify Mott's formula for variable-range hopping [20], where

$$\sigma(T) = \frac{\sigma_0^{/}}{\sqrt{T}} \exp\left[-\left(\frac{T_0}{T}\right)^{1/4}\right]$$

and $T_0 = 16\alpha_0^3/kN(E_F)$. The value of T_0 is a measure of disorder in the material, $\sigma_0^{/}$ is the pre-exponential factor, $N(E_F)$is the density of localized states participating in hopping conduction, α_0 describes the spatial extent of the localization wave function and is assumed to be 0.124 Å^{-1} [21] and k is Boltzmann's constant. Values of $\sigma_0^{/}$, T_0, $N(E_F)$ as well as the room temperature values of hopping distance R and hopping energy W (in Mott's theory $R = [9/(8\pi\alpha kTN(E_F))]^{1/4}$ and $W = 3/4\pi RN(E_F)^3$) were calculated and listed in Table 1. It is clear that the values of $N(E_F)$ increase with increasing the film thickness, which may be attributed to the disorder in In_2O_3 lattice structure due to the increase of the number of unsaturated defects.

The optical band gaps for the films were calculated using equation from the theory of amorphous semiconductors with the extrapolated intercept of the plot $(\alpha h\nu)^2$ versus $h\nu$ [22] as shown in Figure 5a, where α is the absorption coefficient, which can be described as a function of the photon energy $h\nu$:

$$\alpha h\nu \propto (h\nu - E_g)^{1/2}.$$

As seen from Figure 6 the width of the optical band gap E_g decreases with increasing the film thickness from 3.18 to 2.07 eV. This is due to the increase of density of localized states $N(E_F)$.

Figure 7 shows the variation of refractive index and extinction coefficient in the visible region with the film thickness. It is seen that the extinction coefficient can be related to the variation of thickness, where $k = \alpha\lambda/4\pi$. It is obvious also that the refractive index increases with increasing the film thickness, this may be due to the increase of the film density, so the velocity of light in the material will decrease.

In order to enhance the film properties, annealing treatments in air were made in the temperature range from 200 to 400 °C for 15 min and annealing time from 15 to 120 min at 400 °C. The range of annealing temperature from 100 to 200 °C for 15 min was also studied.

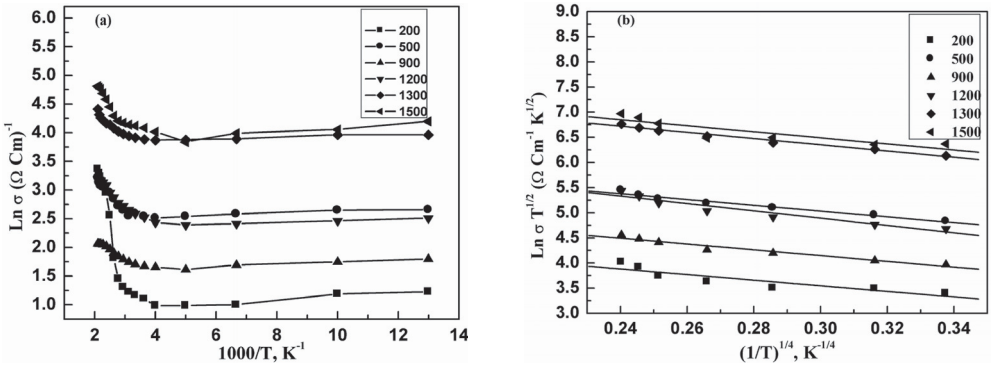

Fig. 4. (a) Ln σ versus $1000/T$ plots as a function of film thickness. (b) Plots of Ln $\sigma T^{1/2}$ versus $(1/T)^{1/4}$ for different film thickness.

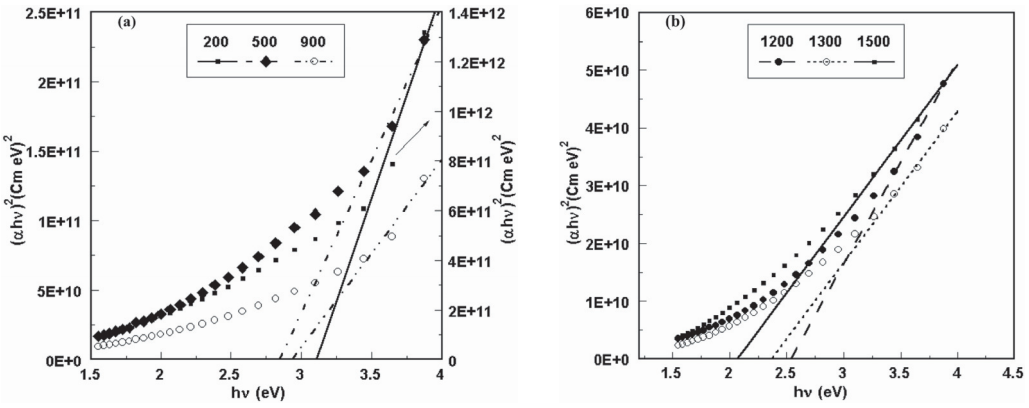

Fig. 5. Plot of $(\alpha h\nu)^2$ vs. $h\nu$ for different film thickness.

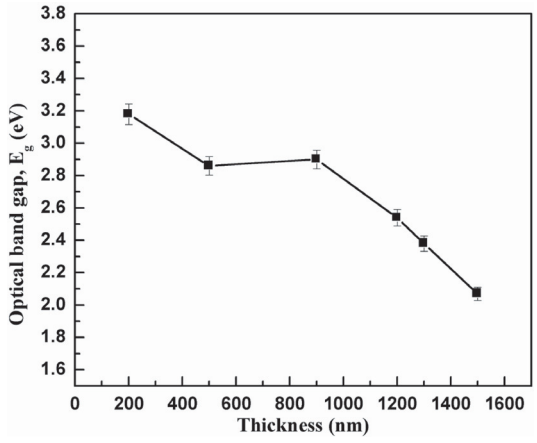

Fig. 6. Plot of the optical band gap E_g as a function of film thickness.

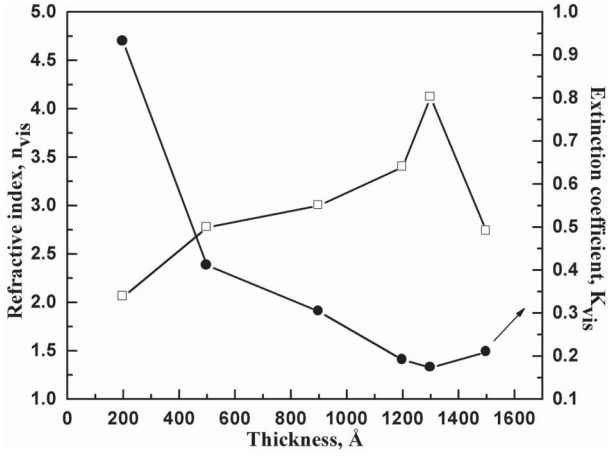

Fig. 7. Variation of the refractive index and the extinction coefficient of the ITO films with different film thickness.

Gessert et al. [23] found that when annealing ITO in air, the crystal size only increased with annealing temperatures above 250 °C. They reported that for vacuum annealing, the grain growth was enhanced for annealing around 350 °C. Some important points should be noted here. When the ITO films in this study were annealed in air at temperatures range from 100 to 200 °C (15 min periods), no change in color was observed. The films remained very dark, exhibiting very low optical transmission. When annealed at 250 °C the optical transmission increased.

Figure 8a presents the effects of annealing temperature on transmittance of ITO films with a thickness of 1500 Å, which were measured in the wavelength range from 200 to 2500 nm. The transmittance in both the visible range and NIR region increased with increasing the annealing temperature and the thermal emissivity decreased with $T_{\rm an}$ as

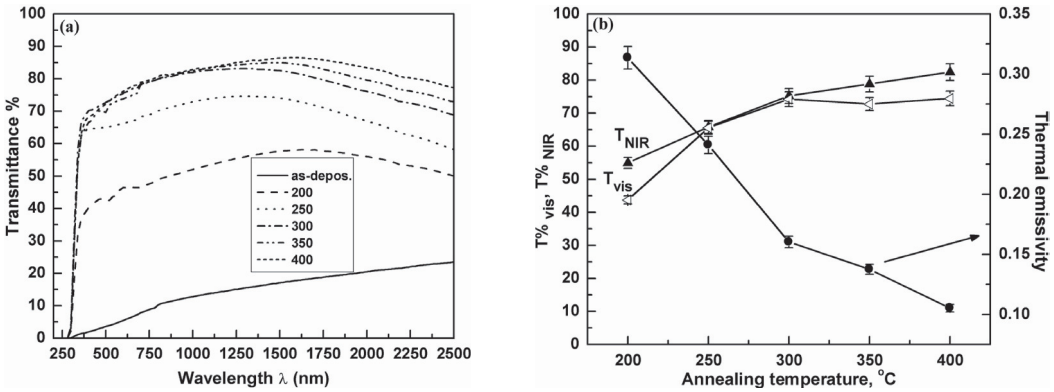

Fig. 8. (a) Spectral variation of the transmittance T with wavelength for 1500 Å film thick at different temperatures for 15 min. (b) Variations of the transmittance in the visible and near infrared region and the thermal emissivity with annealing temperature, $t_{\rm an} = 15$ min and $t = 1500$ Å.

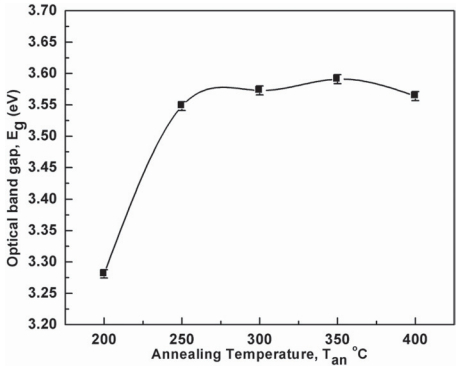

Fig. 9. Variation of the optical band gap E_g with annealing temperature. $t_{\rm an} = 15$ min and $t = 1500$ Å.

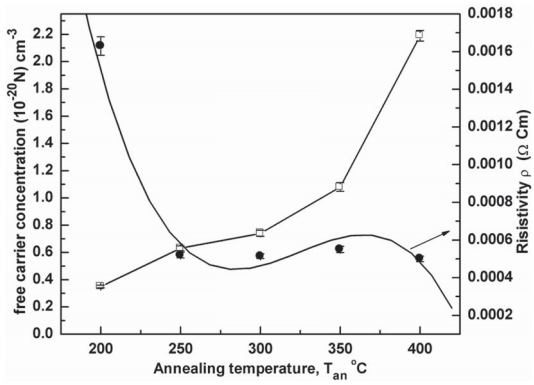

Fig. 10. Variations of the resistivity ρ and the free carrier concentration for ITO films annealed at different temperatures for 15 min.

shown in Figure 8b. It is observed that, before annealing the ITO films, only 20% of incident light was transmitted. For annealed sample with $T_{\rm an} = 400$ °C for 15 min, the average transmission in the visible region goes up to 74%. The transmittance in a region ultraviolet to green light has been much improved. It is obvious that, there was a shift in the absorption edge to shorter wavelength with annealing temperature, which was due to the Burstein-Moss shift [24], indicating a continuous increasing in the energy gap, as shown in Figure 9. This increase in the optical band gap with increasing the temperature of annealing may be due to that the unsaturated defects are gradually annealed out producing a larger number of saturated bonds; this decreases the density of localized states and consequently the optical gap increased.

More significant improvement can also be seen in the results for electrical properties. Figure 10 shows the resistivity $\rho(\Omega$ cm) as a function of annealing temperature and corresponding results for the free carrier concentration N (cm^{-3}), calculated from the optical measurements using Drude's theory as described elsewhere [25,26]. In particular, as the film resistivity decreases, the visual appearance of the films changes optically from very dark brown to transparent. Correspondingly, microstructure changes from amorphous to microcrystalline, and eventually to polycrystalline.

In order to predict the selective properties of transparent conductive coatings from the fundamental optical and electrical properties, the factor of merit φ ($\varphi = T_m/\rho_{RT}$) [27] can be employed, φ has a maximum value when $T_{\rm an} = 400$ °C as shown in Figure 11.

On the other hand, the transmittance T in the wavelength range from 200 to 2500 nm is illustrated in Figure 12 as a function of the annealing time $t$in air at $T_{\rm an} = 400$ °C. It is seen that the average transmission in the visible region improved significantly and goes up to 82%.

The effect of annealing time on the film resistivity ρ measured at room temperature is shown in Figure 13. The resistivity shows an increase with increasing the annealing time up to 15 min, attains a maximum at 45 min and starts decreasing for further increase in time of annealing. This type of behavior is normally observed for disordered materials. Moreover the incorporation of oxygen atoms (due to heat in air) can cause a decrease in current carriers and hence an increase in resistivity. The fall in resistivity can be explained by the improvement in the crystalinity of ITO films with increasing the time of annealing.

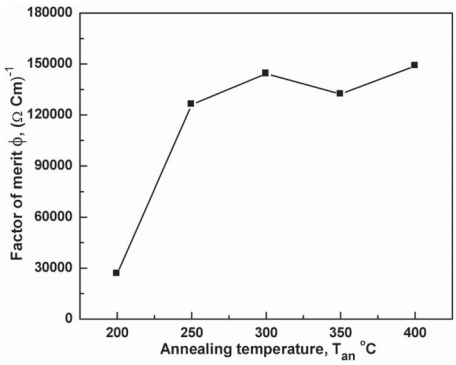

Fig. 11. Annealing temperature dependence of the factor of merit φ for ITO films, $t = 1500$ Å.

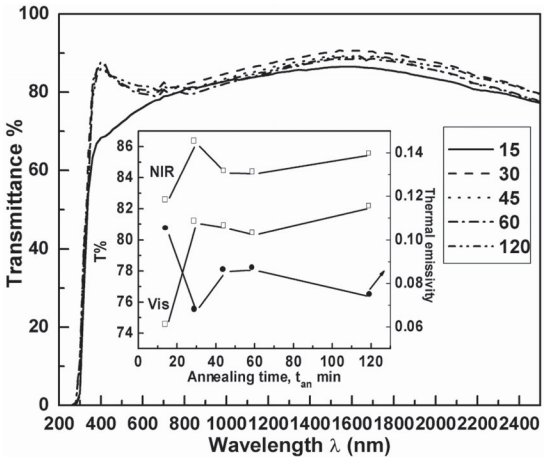

Fig. 12. The spectra of transmittance of ITO films in the wavelength range from 200 to 2500 nm for different annealing time at 400 °C, $t = 1500$ Å.

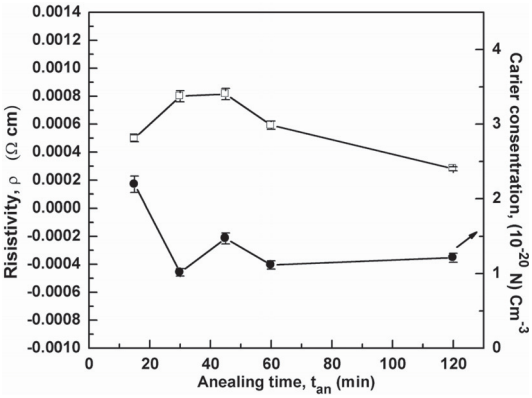

Fig. 13. Plot of the annealing time dependent electrical resistivity ρ and the free carrier concentration for ITO thin films.

The usefulness of a film material to be transparent-conductive material, usually in the visible spectral region, is assessed by its factor of merit φ. As shown in Figure 14, φ, which has a maximum value for 1500 Å film thick annealed at 400 °C for 120 min, can be improved with increasing the time of annealing.

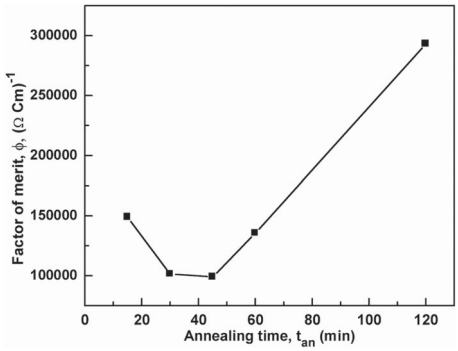

Fig. 14. Annealing time dependence of the factor of merit φ for ITO films, $t = 1500$ Å.

It is important to indicate that the electrical conductivity and the transmittance were measured twice with an interval of three months; during this time samples were exposed to ambient conditions. The conductivity and transmittance showed no variation after this time. This confirms their performance as long-term selective layers.

4 Conclusion

The effect of thickness of ITO thin films deposited onto glass substrates at room temperature by electron beam evaporation technique of a 90% In_2O_3–10% SnO_2 cold pressed powder has been studied. It has been experimentally found that the transmittance and resistivity decrease with increasing the film thickness. We concluded that the optical and electrical properties of ITO thin films are sensitive to film thickness. Annealing was carried out on ITO thin film with 1500 Å to enhance their optical and electrical properties, an average visible transmittance of 74% and an electrical resistivity of $5 \times 10^{-4}(\Omega$ cm) were obtained. Annealing temperature dependence of the factor of merit φ for ITO films suggests that further improvements of conductivity and transmittance in the visible region achieved at $T_{an} = 400$ °C for 15 min. Thus, annealing was performed at this point of temperature for different time. It has been found that, a transmittance value of 85.5% in the IR region and 82% in the visible region of the spectrum and a resistivity of 2.8×10^{-4} (Ω cm) were obtained at $T_{an} = 400$ °C for 120 min. No long-term degradation of conductivity and transmittance was observed.

The authors would like to thank Prof. Dr. M.M. Wakkad and Prof. Dr. M.M. Ibrahim for their continuous encouragement and comments.

References

1. A. El Hichou, A. Kachouane, J.L. Bubendorff, M. Addou, J. Ebothe, M. Troyon, A. Bougrine, Thin Solid Films **458**, 263 (2004)
2. S.H. Brewer, S. Franzen, Chem. Phys. **300**, 285 (2004)

3. H.L. Hartnagel, A.L. Dawar, A.K. Jain, C. Jagadish, *Semiconducting Transparent Thin Films* (Institute of Physics, Bristol, 1995)
4. J.L. Vossen, Phys. Thin Films **9**, 1 (1977)
5. P.K. Biswasa, A. De, N.C. Pramanik, P.K. Chakraborty, K. Ortner, V. Hock, S. Korder, Mater. Lett. **57**, 2326 (2003)
6. G. Frank, E. Kauer, H. Kostlin, Thin Solid Films **77**, 107 (1981)
7. M. Tariq Bhatti, A. Manzoor Rana, Abdul Faheem Khan, Mater. Chem. Phys. **84**, 126 (2004)
8. Y.S. Jung, S.S. Lee, J. Cryst. Growth **259**, 343 (2003)
9. J. Szczyrbowski, A. Dietrich, H. Hoffmann, Phys. Status Solidi A **78**, 243 (1983)
10. M. Buchanan, J.B. Webb, D.F. Williams, Thin Solid Films **80**, 373 (1981)
11. N. Balasubramanian, A. Subrahmanyam, Mater. Sci. Eng. B **1**, 279 (1988)
12. J.L. Yao, S. Hao, J.S. Wilkinson, Thin Solid Films **189**, 227 (1990)
13. S.M. Rozati, T. Ganj, Renew. Energ. **29**, 1671 (2004)
14. B. Bessais, N. Mliki, R. Bennaceur, Semiconductor Sci. Technol. **8**, 116 (1993)
15. J.N. Arfsten, J. Non-Cryst. Solids **63**, 243 (1984)
16. H. Kim, A. Piqué, J.S. Horwitz, H. Mattoussi, H. Murata, Z.H. Kafafi, D.B. Chrisey, Appl. Phys. Lett. **74**, 3444 (1999)
17. E.Kh. Shokr, M.M. Wakkad, H.A. Abd El-Ghanny, H.M. Ali, J. Phys. Chem. Solids **61**, 75 (2000)
18. J.C.C. Fan, J.B. Goodenough, J. Appl. Phys. **48**, 3524 (1977)
19. K. Sreenivas, T. Sundarsena Rao, A. Mansnigh, S. Chandra, J. Appl. Phys. **57**, 384 (1985)
20. N.F. Mott, Philos. Mag. **19**, 835 (1969)
21. H. Fritsche, in *Amorphous and Liquid Semiconductors*, edited by J. Tauc (Plenum, London, 1974), p. 221
22. I.K. El Zawawi, R.A. Abd Alla, Thin Solid Films **339**, 314 (1999)
23. T.A.Gessert, D.L. Williamson, T.J. Coutts, A.J. Nelson, K.M. Jones, R. Dhere et al., J. Appl. Phys. **11**, 60 (1986)
24. E. Burstein, Phys. Rev. **93**, 632 (1954)
25. K. Gurumurugan, D. Mangalaraj, Sa.K. Narayandass, Thin Solid Films **251**, 7 (1994)
26. H. Haitjema, J.J. Ph. Elich, Thin Solid Films **205**, 93 (1991)
27. C. Terrier, J.P. Chatelon, J.A. Roger, Thin Solid Films **295**, 95 (1997)